A Bayesian Model of the DNA Barcode Gap

Jarrett D. Phillips[1,2]* (ORCID: 0000-0001-8390-386X)

[1]*School of Computer Science, University of Guelph, Guelph, ON., Canada, N1G2W1*

[2]*Department of Integrative Biology, University of Guelph, Guelph, ON., Canada, N1G2W1*

*Corresponding Author: Jarrett D. Phillips[1]

Email Address: jphill01@uoguelph.ca

Running Title: Bayesian inference for DNA barcoding

Abstract

Keywords: Bayesian inference, DNA barcoding, intraspecific genetic distance, interspecific genetic distance, specimen identification, species discovery, Stan

1   Introduction

Since its inception over 20 years ago, DNA barcoding (Hebert et al., 2003a,b) has emerged as a robust method of specimen identification and species delimitation across myriad taxonomic groups which have been sequenced at short, standardized gene regions like 5'-COI for animals. However, the success of the approach, particularly for regulatory and forensic applications, depends crucially on two important factors: (1) the availability of high-quality specimen records found in public reference sequence databases such as the Barcode of Life Data Systems (BOLD) (Ratnasingham and Hebert, 2007), and (2) the establishment of a DNA barcode gap — the idea that the maximum genetic distance observed within species is much smaller than the minimum degree of marker variation found among species (Meyer and Paulay, 2005; Meier et al., 2008). Early work has demonstrated that the presence of a DNA barcode gap hinges strongly on extant levels of species haplotype diversity gauged from comprehensive specimen sampling at wide geographic and ecological scales (Bergsten et al., 2012). Despite this, many taxa lack adequate separation in their pairwise intraspecific and interspecific genetic distances, thereby compromising rapid matching of unknown samples to expertly-validated references.

Recent work has argued that DNA barcoding, in its current form, is lacking in statistical rigor, calling into question the existence of a true species' DNA barcode gap (Phillips et al., 2022). To support this notion, novel nonparametric locus-specific metrics based on the multispecies coalescent (Rannala and Yang, 2003; Yang and Rannala, 2017) were recently outlined and shown to hold strong promise when applied to predatory *Agabus* (Coleoptera: Dytiscidae) diving beetles (Phillips et al., 2024), a group, which, despite their morphological uniformity, sre considered to be a taxonomic nightmare. The coalescent (Kingman, 1982) encompasses a backwards continuous-time stochastic Markov process of allelic sampling within natural, neutrally-evolving, species populations towards the Most Recent Common Ancestor (MRCA). The metrics quantify the extent of asymmetric directionality of proportional genetic distance distribution overlap/separation for species within well-sampled taxonomic genera based on a straightforward distance count. The metrics can be employed in a variety of ways, including to assess performance of marker genes for species identication, as well as to assess whether computed values are consistent with population genetic-level parameters like effective population size (N_e), mutation rates (μ) and divergence times (τ) for species under study (Mather et al., 2019). However, what appears to be missing is an unbiased way to compute the statistical accuracy of the recommended estimators arising through problems inherent in frequentist maximum likelihood estimation for discrete probability distributions having bounded positive support on $[0, 1]$. To this end, here, a Bayesian model of the DNA barcode gap coalescent is introduced to rectify such issues. The model allows accurate estimation of posterior means, posterior standard deviations, posterior

⁴⁹ quantiles, and credible intervals for the metrics given datasets of intraspecific and interspecific
⁵⁰ genetic distances for species of interest.

2 Methods

2.1 DNA Barcode Gap Metrics

⁵³ Recently, Phillips et al. (2024) proposed novel nonparametric maximum likelihood
⁵⁴ estimators (MLEs) of proportional overlap/separation between intraspecific and interspecific
⁵⁵ pairwise genetic distance distributions for a given species (x) to aid assessment of the DNA
⁵⁶ barcode gap as follows:

$$p_x = \frac{\#\{d_{ij} \geq a\}}{\#\{d_{ij}\}} \tag{1}$$

$$q_x = \frac{\#\{d_{XY} \leq b\}}{\#\{d_{XY}\}} \tag{2}$$

$$p'_x = \frac{\#\{d_{ij} \geq a'\}}{\#\{d_{ij}\}} \tag{3}$$

$$q'_x = \frac{\#\{d'_{XY} \leq b\}}{\#\{d'_{XY}\}} \tag{4}$$

⁵⁷ where d_{ij} are pairwise genetic distances within species, d_{XY} are genetic distances among
⁵⁸ species for an entire genus of concern, and d'_{XY} are combined interspecific distances for
⁵⁹ a target species and its closest neighbouring species. The notation $\#$ reflects a count
⁶⁰ (**Figure 1**). Quantities a, a', and b correspond to $\min(d_{XY})$, $\min(d'_{XY})$, and $\max(d_{ij})$,
⁶¹ the minimum interspecific distance and the maximum intraspecific distance, respectively.
⁶² Hence, Equations (1)-(4) are simply empirical means of genetic distances falling below or
⁶³ exceeding given distribution thresholds. Notice further that a/a', and b are also the first
⁶⁴ and nth order statistics, respectively. Genetic distances are easily computed from a model
⁶⁵ of DNA sequence evolution, such as uncorrected or corrected p-distances (Jukes and Cantor,
⁶⁶ 1969; Kimura, 1980). If a focal species is found to have multiple nearest neighbours, then
⁶⁷ the species possessing the smallest average pairwise interspecfic distance is used. While these
⁶⁸ schemes differ considerably from the usual definition of the DNA barcode gap laid out by
⁶⁹ Meyer and Paulay (2005) and Meier et al. (2008), they more accurately account for species'
⁷⁰ coalescence histories inferred from contemporaneous samples of DNA sequences, such as
⁷¹ interspecific hybridization/introgression events (Phillips et al., 2024). Note, distances (and
⁷² hence the metrics) are constrained to the closed unit interval $[0, 1]$. Values of the estimators
⁷³ obtained from equations (1)-(4) close to or equal to zero give evidence for separation between
⁷⁴ intraspecific and interspecific genetic distance distributions; that is, values suggest the
⁷⁵ presence of a DNA barcode gap for a target species. Conversely, values near or equal to one
⁷⁶ give evidence for distribution overlap; that is, values likely indicate the absence of a gap.
⁷⁷ Equations (1)-(4) can be expressed in terms of empirical cumulative distribution functions
⁷⁸ (ECDFs) as follows, since the true underlying CDFs, $F(\cdot)$, are unknown

$$p_x = \mathbb{P}(d_{ij} \geq a) \quad = 1 - \hat{F}_{d_{ij}}(a) = \hat{F}_{d_{ij}}(b) - \hat{F}_{d_{ij}}(a) \tag{5}$$

$$q_x = \mathbb{P}(d_{XY} \leq b) = \hat{F}_{d_{XY}}(b) \tag{6}$$

$$p'_x = \mathbb{P}(d_{ij} \geq a') \quad = 1 - \hat{F}_{d_{ij}}(a') = \hat{F}_{d_{ij}}(b) - \hat{F}_{d_{ij}}(a') \tag{7}$$

$$q'_x = \mathbb{P}(d'_{XY} \leq b) = \hat{F}_{d'_{XY}}(b) \tag{8}$$

noting that $\hat{F}_{d_{ij}}(b) = 1$, $\hat{F}_{d_{XY}}(a) = 0$, and $\hat{F}_{d'_{XY}}(a') = 0$ (**Figure 1**). Given n increasing-ordered data points, the ECDF $\hat{F}_n(t) = \frac{1}{n} \sum_{i=1}^{n} \mathbb{1}_{[x_i \leq t]}$ comprises a step function having jump discontinuities of size $\frac{1}{n}$ at each sample observation (x_i), excluding ties (or steps of $\frac{i}{n}$ with tied observations), where $\mathbb{1}(x)$ is the indicator function. Equations (5)-(8) clearly demonstrate the asymmetric directionality of the metrics. Furthermore, calculation of the DNA barcode gap estimators given herein is straightforward as they implicitly account for both total distribution area and overlap, which would each require the use of numerical integration techniques or Monte Carlo simulation.

2.2 A Bayesian Implementation

A major criticism of large sample (frequentist) theory is that it relies on asymptotic properties of the MLE (which is assumed to be a fixed but unknown quantity), such as estimator normality and consistency. This problem is especially pronounced in the case of binomial proportions. The estimated Wald SE of the sample proportion, is given by

$$\widehat{SE[\hat{p}]} = \sqrt{\frac{\hat{p}(1 - \hat{p})}{n}}, \tag{9}$$

where $\hat{p} = \frac{Y}{n}$ is the MLE, Y is the number of successes ($Y = \sum_{i=1}^{n} y_i$) and n is the number of trials (*i.e.*, sample size). However, the above formula is problematic for several reasons. First, Equation (9) makes use of the Central Limit Theorem (CLT); thus, large sample sizes are required for reliable estimation. When few observations are available, SEs will be large and inaccurate, leading to low statistical power. Further, resulting interval estimates could span values less than zero or greater than one, or have zero width, which is practically meaningless. Second, when proprtions are exactly equal to zero or one, resulting SEs will be exactly zero, rendering Equation (9) completely useless. In the context of the proposed DNA barcode gap metrics, values obtained at the boundaries of their support are often encountered. Therefore, reliable calculation of SEs is not feasible. Given the importance of sufficient sampling of species genetic diversity for DNA barcoding initiatives, a different statistical estimation approach is necessary. Bayesian inference offers a natural path forward in this regard since it allows for straightforward specification of prior beliefs concerning unknown model parameters and permits the seamless propagation of uncertainty, when data is lacking, through integration with the likelihood function associated with true generating processes. As a consequence, because parameters are treated as random variables, Bayesian models are much more flexible and generally more easily interpretable compared to frequentist approaches since, under the latter paradigm, entire posterior distributions, along with their

110 summaries, are outputted, rather than just sampling distributions, p-values, and confidence
111 intervals as in the former case, thus allowing direct probability statements to be made.

2.3 The Model

113 Essentially, from a statistical perspective, the goal herein is to nonparametrically estimate
114 probabilities corresponding to extreme tail quantiles for positive highly skewed distributions
115 on the unit interval. Here, it is sought to numerically approximate the extent of
116 overlap/separation of intraspecific and interspecific pairwise genetic distance distributions
117 within $[a, b]$. This is a challenging computational problem within the current study as detailed
118 in subsequent sections. The usual approach employs Kernel Density Estimation (KDE),
119 along with numerical integration; however, this requires careful selection of the bandwidth
120 parameter. Here, for simplicity, a different route is taken. Counts, y, of overlapping genetic
121 distances (as expressed in the numerator of Equations (1)-(4)) are treated as binomially
122 distributed with expectation $\mathbb{E}[Y] = k\theta$, where $k = \{N, C\}$ are total count vectors of
123 intraspecific and combined genetic distances, respectively, for a target species along with
124 its nearest neighbour species, and $k = M$ is a total count vector for all pairwise species
125 comparisons. The quantity $\theta = \{p_x, q_x, p'_x, q'_x\}$. The metrics encompassing θ are presumed
126 to follow a beta(α, β) distribution, with real shape parameters α and β, which is a natural
127 choice of prior on probabilities. Such a scheme is quite convenient since the beta distribution
128 is conjugate to the binomial distribution. Thus, the posterior distribution is also beta
129 distributed. Parameters were given an uninformative Beta(1, 1) prior, which is equivalent to
130 a standard uniform (Uniform(0, 1)) prior since it places equal probability on all parameter
131 values within its support. As a result, the posterior is Beta$(Y + 1, n - Y + 1)$, from which
132 various moments and other quantities, such as the expected value $\mathbb{E}[Y] = \frac{Y+1}{n+2}$ and variance
133 $\mathbb{V}[Y] = \frac{(Y+1)(n-Y+1)}{(n+2)^2(n+3)}$, can be easily calculated. In general however, when possible, it is
134 always advisable to incorporate prior information, even if only weak, rather than simply
135 imposing complete ignorance in the form of a flat prior distribution. With sufficient data,
136 the choice of prior distribution becomes less important since the posterior will be dominated
137 by the likelihood. The full univariate Bayesian model for species x is thus given by

$$\begin{aligned}
y_{\text{lwr}} &\sim \text{Binomial}(N, p_{\text{lwr}}) \\
y_{\text{upr}} &\sim \text{Binomial}(M, p_{\text{upr}}) \\
y'_{\text{lwr}} &\sim \text{Binomial}(N, p'_{\text{lwr}}) \\
y'_{\text{upr}} &\sim \text{Binomial}(C, p'_{\text{upr}}) \\
p_{\text{lwr}}, p_{\text{upr}}, p'_{\text{lwr}}, p'_{\text{upr}} &\sim \text{Beta}(1, 1).
\end{aligned} \tag{10}$$

138 The model, which is inherently vectorized to allow processing of multiple species datasets
139 simultaneously, was fitted using the Stan probabilistic programming language (Carpenter
140 et al., 2017) framework for Hamiltonian Monte Carlo (HMC) via the No-U-Turn Sampler
141 (NUTS) sampling algorithm (Hoffman and Gelman, 2014) through the `rstan` R package (Stan
142 Development Team, 2023). Four chains were run for 2000 iterations each in parallel across
143 four cores with random parameter initializations. Within each chain, a total of 1000 samples

was discarded as warmup (*i.e.*, burnin) to reduce dependence on starting conditions. Further, 1000 post-warmup draws were utilized per chain. Because HMC/NUTS results in dependent samples that are minimally autocorrelated, Markov chain thinning is not required. Each of these reflect default MCMC settings in Stan. Since the DNA barcode gap metrics often attain values very close to zero and/or very near one, in addition to more intermediate values, a noninformative $\text{Beta}(\frac{1}{2}, \frac{1}{2})$ prior, which is U-shaped symmetric and places greater probability density at the extremes of the distribution due to its heavier tails, while still allowing for variability in parameter estimates within intermediate values along its domain, was also attempted. However, this resulted in several divergent transitions, among other pathologies, imposed by complex geometry (*i.e.*, curvature) in the posterior space, despite remedies to resolve them, such as lowering the step size of the HMC/NUTS sampler. Note that this prior is Jeffreys' prior, which is proportional to the square root of the Fisher information and has several desirable statistical properties, most notably invariance to reparameterization.

To validate the overall correctness of the proposed statistical model given by Equation (10), in addition to generating MLEs as a means of comparison, posterior predictive checks were also employed to generate binomial random variates in the form of counts from the posterior predictive distribution; that is $\gamma = \{Np_x, Mq_x, Np_x', Cq_x'\}$ to verify that the model adequately captures relevant features of the observed data.

2.4   Model Interpretation

The proposed Bayesian model outlined herein has a straightforward interpretation (**Table 1**). Framed more succinctly,

- If b is relatively large and a is relatively small, p_{lwr} represents the extent to which intraspecific distances tend to be larger than interspecific distances at and beyond a and at and below b;

- If a is relatively large and b is relatively small, p_{upr} represents the extent to which interspecific distances tend to be larger than intraspecific distances at and below b and at and beyond a;

- If b is relatively small and a' is relatively large, p_{lwr}' represents the extent to which intraspecific distances tend to be larger than combined interspecific distances for a target species and its nearest neighbour species at and beyond a' and at and below b; and,

- If a' is relatively small and b is relatively large, p_{upr}' represents the extent to which combined interspecific distances for a target species and its nearest neighbour species tend to be larger than intraspecific distances at and below b and at and beyond a'.

2.5   Case Study

3   Results

4   Discussion

5   Conclusion

Supplementary Information

Information accompanying this article can be found in Supplemental Information.pdf.

Data Availability Statement

Raw data, R, and Stan code can be found on GitHub at:
https://github.com/jphill01/Bayesian-DNA-Barcode-Gap-Coalescent.

Acknowledgements

Funding

Conflict of Interest

None declared.

Author Contributions

JDP wrote the manuscript, wrote R and Stan code, approved all developed code as well as analysed and interpreted all experimental results.

References

Bergsten, J., D. Bilton, T. Fujisawa, M. Elliott, M. Monaghan, M. Balke, L. Hendrich, J. Geijer, J. Herrmann, G. Foster, I. Ribera, A. Nilsson, T. Barraclough, and A. Vogler 2012. The effect of geographical scale of sampling on DNA barcoding. *Systematic biology*, 61(5):851–869.

Carpenter, B., A. Gelman, M. Hoffman, D. Lee, B. Goodrich, M. Betancourt, M. Brubaker, J. Guo, P. Li, and A. Riddell 2017. Stan: A probabilistic programming language. *Journal of Statistical Software*, 76:1.

Hebert, P., A. Cywinska, S. Ball, and J. deWaard

2003a. Biological identifications through DNA barcodes. *Proceedings of the Royal Society of London B: Biological Sciences*, 270(1512):313–321.

Hebert, P., S. Ratnasingham, and J. de Waard

2003b. Barcoding animal life: cytochrome c oxidase subunit 1 divergences among closely related species. *Proceedings of the Royal Society of London B: Biological Sciences*, 270(Suppl 1):S96–S99.

Hoffman, M. and A. Gelman

2014. The No-U-Turn Sampler: Adaptively setting path lengths in Hamiltonian Monte Carlo. *Journal of Machine Learning Research*, 15:1593–1623.

Jukes, T. and C. Cantor

1969. Evolution of protein molecules. In *Mammalian Protein Metabolism*, H. N. Munro, ed., Pp. 21–132. New York: Academic Press.

Kimura, M.

1980. A simple method for estimating evolutionary rates of base substitutions through comparative studies of nucleotide sequences. *Journal of Molecular Evolution*, 16(1):111–120.

Kingman, J.

1982. The coalescent. *Stochastic Processes and Their Applications*, 13:235–248.

Mather, N., S. Traves, and S. Ho

2019. A practical introduction to sequentially Markovian coalescent methods for estimating demographic history from genomic data. *Ecology and Evolution*, 10(1):579–589.

Meier, R., G. Zhang, and F. Ali

2008. The use of mean instead of smallest interspecific distances exaggerates the size of the "barcoding gap" and leads to misidentification. *Systematic Biology*, 57(5):809–813.

Meyer, C. and G. Paulay

2005. DNA barcoding: error rates based on comprehensive sampling. *PLOS Biology*, 3(12):e422.

Phillips, J., D. Gillis, and R. Hanner

2022. Lack of statistical rigor in DNA barcoding likely invalidates the presence of a true species' barcode gap. *Frontiers in Ecology and Evolution*, 10:859099.

Phillips, J., C. Griswold, R. Young, N. Hubert, and H. Hanner

2024. *A Measure of the DNA Barcode Gap for Applied and Basic Research*, Pp. 375–390. New York, NY: Springer US.

Rannala, B. and Z. Yang

2003. Bayes estimation of species divergence times and ancestral population sizes using dna sequences from multiple loci. *Genetics*, 164:1645–1656.

247 Ratnasingham, S. and P. Hebert

248   2007. BOLD: The Barcode of Life Data System (http://www. barcodinglife. org). *Molecular*

249   *Ecology Notes*, 7(3):355–364.

250 Stan Development Team

251   2023. RStan: The R interface to Stan. R package version 2.21.8.

252 Yang, Z. and B. Rannala

253   2017. Bayesian species identification under the multispecies coalescent provides significant

254   improvements to DNA barcoding analyses. *Molecular Ecology*, 26:3028–3036.

255 # Figures and Tables
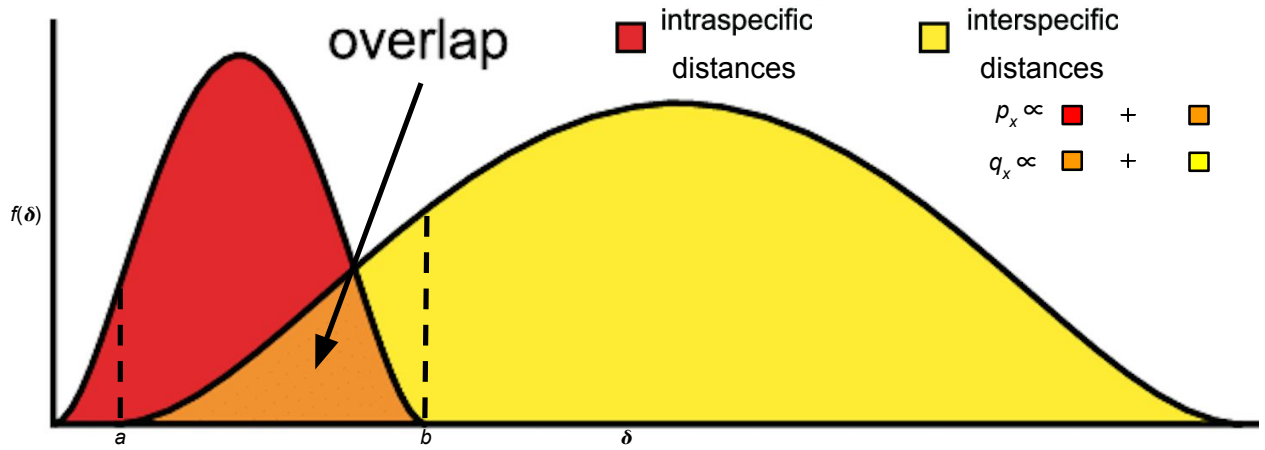
Figure 1: Modified depiction from Meyer and Paulay (2005) and Phillips et al. (2024) of the overlap/separation of pairwise intraspecific and interspecific genetic distances (δ) for calculation of the DNA barcode gap metrics (p_x and q_x) for a hypothetical species x. The minimum interspecific distance is denoted by a and the maximum intraspecific distance is indicated by b. The quantity $f(\delta)$ is akin to a kernel density estimate of the probability density function of pairwise genetic distances. A similar visualization can be displayed for $p_x^{'}$ and $q_x^{'}$.

Table 1: Interpretation of the Model

Parameter	Explanation
p_{lwr}	When p_{lwr} is close to 0 (1), it suggests that the probability of intraspecific (interspecific) distances being larger (smaller) than interspecific (intraspecific) distances is low (high) on average, while the probability of interspecific (intraspecific) distances being larger (smaller) than intraspecific (interspecific) distances is high (low) on average; that is, there is (no) evidence for a DNA barcode gap.
p_{upr}	When p_{upr} is close to 0 (1), it suggests that the probability of interspecific (intraspecific) distances being larger (smaller) than intraspecific (interspecific) distances is high (low) on average, while the probability of intraspecific (interspecific) distances being larger (smaaler) than interspecific (intraspecfic) distances is low (high) on average; that is, there is (no) evidence for a DNA barcode gap.
p'_{lwr}	When p'_{lwr} is close to 0 (1), it suggests that the probability of intraspecific (combined interspecific distances for a target species and its nearest neighbour species) distances being larger than combined interspecific distances for a target species and its nearest neighbour species (intraspecific distances) is low (high) on average, while the probability of combined interspecific distances for a target species and its nearest neighbour species (intraspecfic distances) being larger than intraspecific distances (combined interspecific distances for a target species and its nearest neighbour species) is high (low) on average; that is, there is (no) evidence for a DNA barcode gap.
p'_{upr}	When p'_{upr} is close to 0 (1), it suggests that the probability of combined interspecific distances for a target species and its nearest neighbour species (intraspecific distances) being larger than intraspecific distances (combined interspecific distances for a target species and its nearest neighbour species) is high (low) on average, while the probability of intraspecific distances (combined interspecific distances for a target species and its nearest neighbour species) being larger than combined interspecific distances for a target species and its nearest neighbour species (intraspecific distances) is low (high) on average; that is, there is (no) evidence for a DNA barcode gap.